Solitary Waves and Fluctuations in Fragile Matter

Upadhyaya, N.

6

SHEAR FRONTS IN RANDOM SPRING NETWORKS

As discussed in the introduction, a disordered network of harmonic springs constitutes another interesting model for fragile matter, where the loss of rigidity is a collective phenomenon. In this chapter, we turn to the study of this model by subjecting a two dimensional random network of harmonic springs (not coupled to any other local source of fluctuations) to a constant influx of energy, by shearing one of its edges at a uniform rate. We will then study the response of the network by following the evolution and propagation of the resulting shear excitations.

We construct computer models of weakly connected two dimensional random viscoelastic networks from highly compressed jammed packings of frictionless poly-disperse disks. One first identifies the disk centers as point particles (network nodes) and then models the interactions between overlapping disks using two sided harmonic springs of varying rest length to eliminate any pre-stress existing in the original jammed packings. The result is a highly coordinated ($z \approx 6$) spring network that serves as the seed from which families of networks with a wide range of z are generated by removing springs. See, Fig. (6.1).

Once the networks are generated, we shear the left most edge at a constant speed v_0, and follow the evolution of the resulting shear velocity profile by averaging out the longitudinal particle speeds over bins along the x direction effectively creating a one dimensional front profile propagating in the x direction. Note here, it is useful to express the rate of shearing in terms of dimensionless parameter, that we define as the strain $\gamma = \frac{v_0}{v_f}$, where v_f is the speed of propagation of the front. In the following discussions, we will find two distinct regimes of shear front propagation - a linear regime for $\gamma < \gamma_c$ and a non-linear regime for $\gamma > \gamma_c$, where γ_c is the critical strain, to be defined later.

The dynamics is obtained by numerically integrating Newton's equations of motion (using the velocity Verlet method) subject to Lees-Edwards boundary conditions in the y-direction

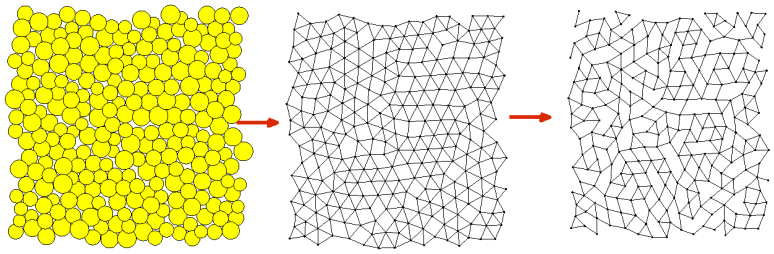

Figure 6.1: From a jammed packing of soft frictionless disks (left), we identify the disk centers with point nodes and model the interaction between overlapping disks as harmonic springs (middle). We then remove springs to obtain an ensemble of disordered spring networks with the desired coordination number (right).

and hard walls in the x-direction *. The samples are composed of up to $N = 10^5$ identical particles with mass m. In addition to the Hookean interaction (with a spring constant k) between connected particles, i, j, we include the effects of viscous dissipation: $\vec{f}^{ij}_{diss} = -b(\vec{v}^i - \vec{v}^j)$, where b is the microscopic damping constant, and $\vec{v}^{i,j}$ are the velocities of a pair of particles connected by a spring. Time is measured in units of $\sqrt{m/k}$ and the damping constant in units of $\sqrt{km}$, which is equivalent to setting $m = 1$ and $k = 1$. Lengths are measured in units of d the mean spring length at rest.

6.1 LINEAR REGIME

6.1.1 *Early time*

In the inset to Fig. (6.2), we plot the resulting velocity field (normalized by the shearing rate v_0) for times less than a critical transition time , i.e., $t < t_c$. Notice, the velocity field simply broadens away from the shearing edge that is located at x=0, while remaining centered there. Thus, in this regime, we do not observe any propagating shear fronts.

In the main panel of Fig. (6.2), we plot the width $w(t)$ of the velocity field as a function of time t. Expectedly, the width in-

* A hard wall can only move up and down as a whole, but no relative motion of the particles is allowed.

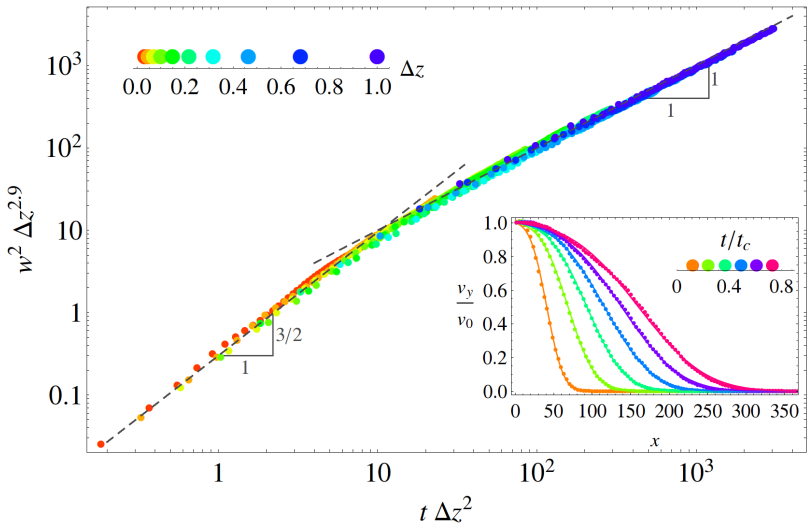

Figure 6.2: The main plot shows the time evolution of the squared front width, whereby the time axis has been normalized by $t_c \propto \Delta z^{-2}$ and the width axis by $\Delta z^{2.9}$. The inset shows the broadening at early times, $t < t_c$, of the velocity profiles, $v(x,t)$, in the $\hat{y}$ direction, normalized by v_0. Note the absence of front *propagation*, in contrast with the plot in the left inset of Fig. (6.3).

creases with time. At early times we find that $w^2 dz^3 \sim (t dz^2)^{\frac{3}{2}}$, implying, a super-diffusively increasing width:

$$w^2(t) \sim t^{\frac{3}{2}}. \tag{6.1}$$

However, at later times ($t > t_c$), there is a transition to a new regime where the width increases diffusively,

$$w^2(t) \sim \frac{t}{dz}. \tag{6.2}$$

Recall, particle diffusion in a medium can be characterized by a diffusion constant defined from the mean square displacement as:

$$\langle r^2(t) - r^2(0)\rangle = D t^{\xi}, \tag{6.3}$$

where, $r(t)$ is the displacement, D is a characteristic diffusion constant and ξ is an exponent characterizing the nature of diffusion. If $\xi = 1$, we are in the regime of normal diffusion where the mean square displacement increases linearly with time and is consistent with the late time dynamics that we observe in Fig. (6.2) and Eq. (6.2). By contrast, a ξ different from 1 is considered

anomalous diffusion, with $\xi < 1$ being referred to as the sub-diffusive regime and $\xi > 1$ as the regime of super-diffusion. From Eq. (6.1), we find that a $\xi = \frac{3}{2}$ characterizes the broadening of the velocity field at early times.

In the super-diffusive regime, Eq. (6.3) can also be interpreted in the form

$$\langle r^2(t) - r^2(0)\rangle = D(t)t, \tag{6.4}$$

with a diffusivity that depends upon time ,i.e., $D(t) = Dt^{\xi-1}$ (see also Chapter 4). If $\xi > 1$, this implies that the diffusivity will continue to increase with time. However, we note from Fig. (6.2) that beyond a transition time t_c we enter the regime of normal diffusion that has a constant diffusivity. Thus, if we imagine that this transition process physically corresponds to a diffusivity that increases with time until it saturates to a constant value $\frac{1}{dz}$ (from Eq. (6.2)), we find the transition time,

$$Dt^{\xi-1} \sim \frac{1}{dz} \tag{6.5}$$

$$t \sim \left(\frac{1}{dz}\right)^{\frac{1}{\xi-1}}. \tag{6.6}$$

For $\xi = \frac{3}{2}$,the transition time is therefore

$$t_c \sim \frac{1}{dz^2}. \tag{6.7}$$

This explains the choice of normalization used in the axes of Fig. (6.2). Note, the critical transition time is exactly the critical time for transition from the so called non-quasistatic regime to the quasi-static regime, first studied for visco-elastic random spring networks using linear oscillatory rheology [4].

In the context of the transverse velocity field studied here, physically, the transition time represents the time required for the front width to increase to a large enough length scale so that wave numbers characterizing the front discontinuity only contains low frequency components and the network response can then be described by frequency independent elastic constants. The length scale up to which anomalous diffusion persists is then

$$l_c \sim t_c^{\frac{3}{4}} \sim \frac{1}{dz^{\frac{3}{2}}}. \tag{6.8}$$

This length scale can therefore be associated with the characteristic size of the network beyond which its response can be considered elastic, as we will see in the next section.

6.1.2 *Late Times*

At late times (for $t > t_c$), along with the transition to a regime where the width spreads diffusively, we also find the onset of front propagation, see inset to Fig. (6.3), with a speed that is characteristic of the network shear modulus. As discussed in the introductory chapter, for random spring networks near the rigidity transition critical point, the shear modulus scales linearly with the excess coordination number $G \sim dz$. In Fig. (6.4), we extract from the speed of front propagation, the corresponding shear modulus via the relation $c_s \sim \sqrt{G}$, and plot it as a function of dz, finding very good agreement with the expected scaling.

In addition, in Fig. (6.5), we extract the width of the propagating shear fronts as a function of dz (after normalizing out the diffusive spreading in time seen in Fig. (6.2). As anticipated from the relation Eq. (6.2), we find a width that diverges with the excess coordination number $w^2 \sim \frac{1}{dz}$. Conversely, from the width of the propagating fronts we can define a transport coefficient, that we call the effective viscosity of the network $\eta_e \sim \frac{1}{dz}$. Phenomenologically, this amounts to a second order equation of motion for the transverse y- displacement field of the form

$$\rho \frac{\partial^2 y}{\partial t^2} = G \frac{\partial^2 y}{\partial x^2} + \eta_e \frac{\partial^3 y}{\partial x^2 \partial t}. \tag{6.9}$$

In turn, this equation can be derived from a visco-elastic stress-strain relation of the form:

$$\sigma = G\gamma + \eta_e \dot{\gamma}, \tag{6.10}$$

where $\gamma = \frac{\partial y}{\partial x}$. Thus, for $t > t_c$, the network response can be effectively described by time independent (or frequency independent) characteristic storage (G) and loss (η_e) moduli. As discussed in the introductory chapter, this is consistent with the recent studies that probe random visco-elastic spring networks by imposing a linear frequency dependent strain at the boundaries (oscillatory rheology), where the response of the networks in the quasi-static regime (for frequencies $\omega < \omega_c \sim dz^2$) is characterized by frequency independent storage modulus $G \sim dz$ and a frequency independent loss modulus $\eta \sim \frac{1}{dz}$. By contrast, for $\omega > \omega_c$, the complex moduli are frequency dependent. See Supplementary information F for more details, including a derivation of the velocity profiles in the frequency dependent regime.

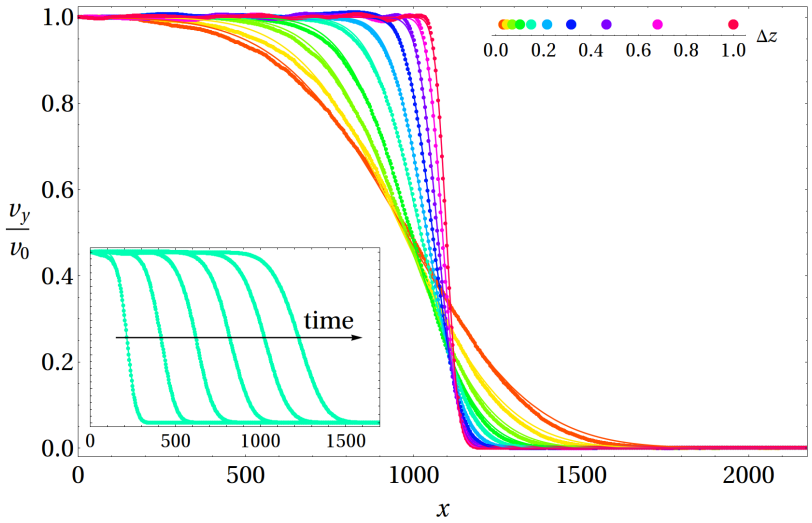

Figure 6.3: Shape of the linear wave profile. In the main plot, velocity profiles for different Δz are superimposed, with the smallest Δz corresponding to the widest profile. The damping coefficient is $b = 0.1$ and the time is chosen such that the wave has roughly reached the center of the sample. The left inset shows the wave front for $\Delta z = 0.15$ (same color as main plot) for different times. In all plots, data points are (averaged) profiles from the simulation and the solid lines are fits to analytical solution [9].

6.2 NON-LINEAR REGIME

For large strain rates i.e., $\gamma > \gamma_c$ the network response changes substantially, see Fig. (6.6). Compared to the inset in Fig. (6.2), we now find that even at early times, a well defined front propagates. At the same time, the front width continues to increase super diffusively with the same exponent $\xi = \frac{3}{2}$ as seen in the linear regime. However, unlike the case for $\gamma < \gamma_c$ where we found a cross-over to ordinary diffusion for times $t > t_c$, we no longer observe such a transition in the non-linear regime during the entire times probed in our simulations, see Fig. (6.7).

For a qualitative understanding of this network response for large strains, consider first, the one dimensional diffusion equation :

$$\frac{\partial u}{\partial t} = D\frac{\partial^2 u}{\partial^2 x}. \tag{6.11}$$

Let us impose a field of the form $u = u_0 e^{i(kx-\omega t)}$. The solution is:

$$u = u_0 e^{\left(\frac{-t}{t_r}\right)} e^{ikx}, \tag{6.12}$$

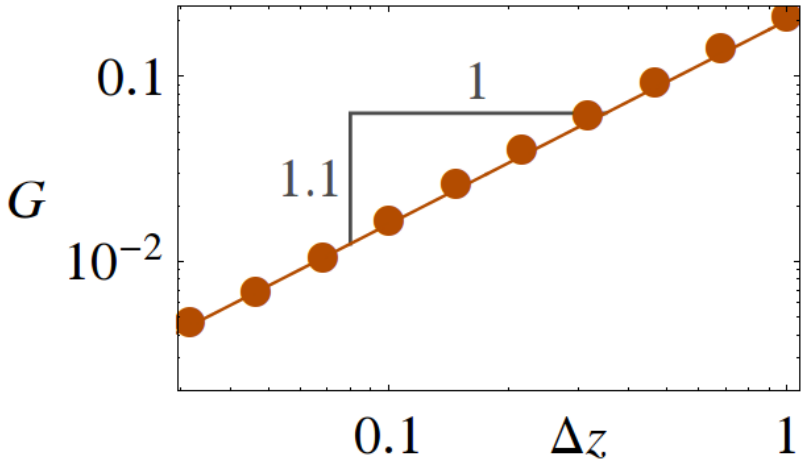

Figure 6.4: The shear modulus G versus Δz extracted from the speed of the linear front propagating in a homogeneously cut network.

where we have defined a response time t_r

$$t_r = \frac{1}{Dk^2}. \tag{6.13}$$

This implies that for large wave numbers (or small wavelength fluctuations), the response time for their decay is very small. However, at such short time scales, the continuum diffusion equation Eq. (6.11) should no longer be a good approximation to the physical processes since the diffusion equation is generally associated with the long wavelength and long time properties of the medium. In fluids for instance, one way to account for the short time response of the fluid is to introduce a diffusion kernel (memory function) [69]. Similarly, the anomalous wavenumber dependent viscosity that we observed in the quasi-equilibrium state of amorphous packings (see Chapter 4) is also related to the inability of fluids in low dimensions to respond instantaneously to fluctuations. Since the transport properties (such as diffusivity, viscosity, conductivity) are long time integrals of correlation functions, their time dependence typically correspond to correlation functions that do not decay exponentially but have a long time power law tail.

Similarly for the random spring networks, we find that their initial response in the linear regime is marked by a diffusivity that is time (frequency) dependent. Only when the diffusion causes the width to grow to large enough length scales of the order of l_c (small wave numbers), do we find a transition to a

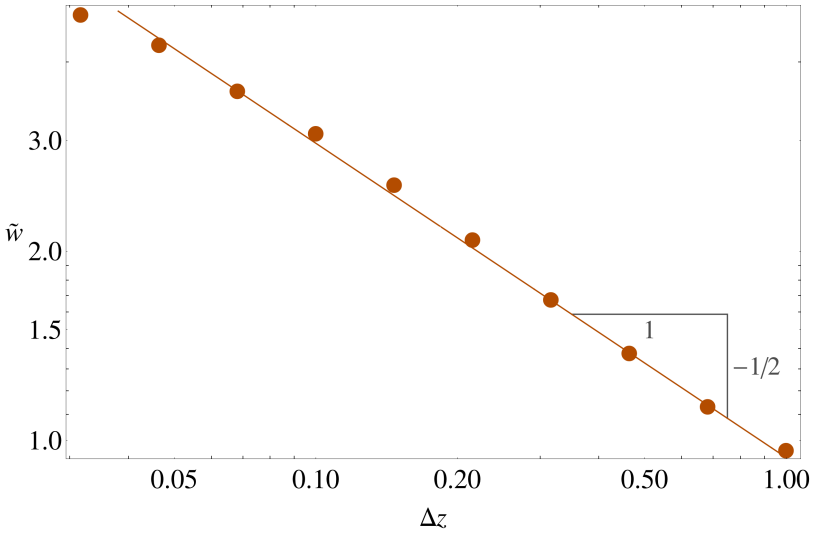

Figure 6.5: The main panel shows numerical data for the rescaled width $\tilde{w} \equiv \frac{w(t)}{\sqrt{t}}$ (or equivalently the effective viscosity η_e) versus Δz (dots) for homogeneously cut networks with $b = 0.1$. The solid line represents the scaling $\tilde{w} \propto \Delta z^{-\frac{1}{2}}$.

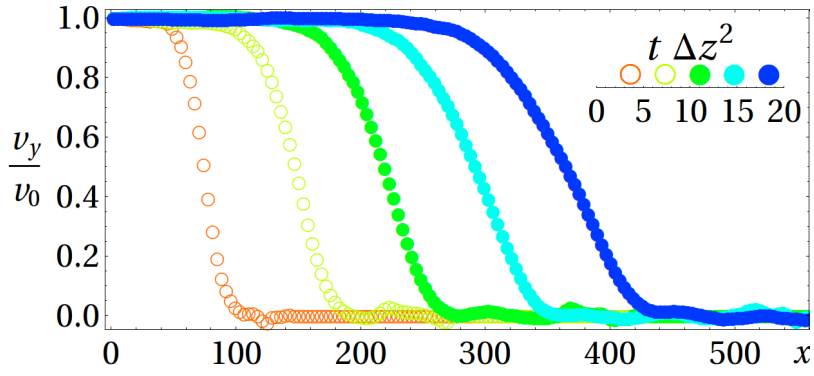

Figure 6.6: Evolution of a non-linear ($\frac{\gamma}{\gamma_c} = 6.8$) wave front for $\Delta z \approx 0.15$. Late times $t\Delta z^2 > 10$ are indicated by full circles.

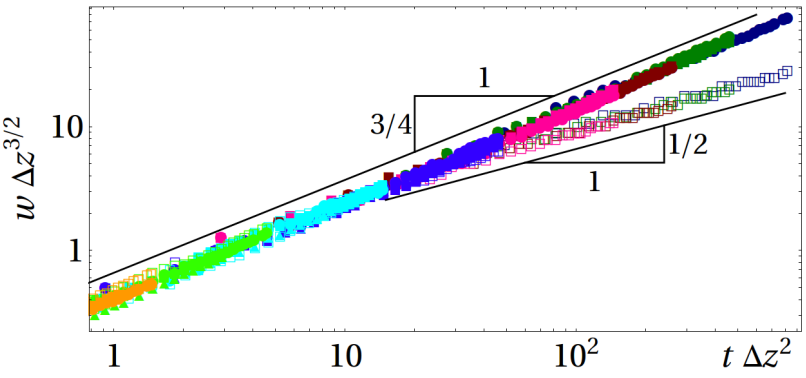

Figure 6.7: Time dependence of the widths in the non-linear regime. Different colors correspond to different Δz, as in the plot on the left. The full symbols correspond to the non-linear regime with $1.5 < \frac{\gamma}{\gamma_c} < 680$. The open symbols correspond to the linear regime $\left(\frac{\gamma}{\gamma_c} < 10^{-3}\right)$.

regime where the transport process with a constant diffusivity may be defined. However, why is this regime not attained when the strain rates are large ?

Intuitively, for large strain rates, Eq. (6.11) is expected to be modified to include non-linear corrections of the form:

$$\frac{\partial u}{\partial t} + \kappa \frac{\partial u^n}{\partial x} = D \frac{\partial^2 u}{\partial^2 x}, \tag{6.14}$$

where n is the index of non-linearity.

Consider the simplest non-linear term with $n = 2$ (such as in the Navier-Stokes equation without a pressure gradient term). How does this term respond to a perturbation of the form : $u = u_0 \cos(kx)$, that we considered previously. To leading order, we find $u^2 = u_0^2 \cos^2 kx$ and upon differentiating once with respect to the spatial variable x, we find a new term of the form $u_0^2 \sin(2kx)$ with a wavenumber $2k$. Once a perturbation with larger wavenumber is generated, the non-linear term responds again to this new perturbation, by generating another higher wavenumber, and this process thus keeps repeating, limited only by the largest wavenumber physically supported by the medium or by other dissipative processes. Thus, one effect of the non-linear term is that it acts as a source term that generates higher wavenumbers. This mechanism is similar to the generation of smaller and smaller eddies in the study of turbulence, where large wavenumbers represent the smaller eddies that are eventually dissipated by thermal processes, such as the one encapsulated in Eq. (6.13).

Thus, if the response of random spring networks at high strain rates is non-linear, then one effect of the non-linearity would be to act as a source for higher wave numbers. However, Eq. (6.13) also indicates that due to the generation of the higher wave numbers, the network will have to keep responding at short time scales to diffusive these fluctuations away. This, in a sense is the physical process modelled by Eq. (6.14). However, at short time scales, the response of random spring networks is no longer in the quasi-static regime with a constant diffusivity D and therefore, the non-linearity constantly forces the system to remain in the regime with a time dependent diffusivity. By contrast, in the linear regime, once the higher wave-numbers inevitably generated during the early phases of the network response (due to the sharper front discontinuities) have been dissipated away, the network gradually enters the regime of quasi-static visco-elastic response with constant material properties.

Is there a distinctive signature of the kind of non-linearity present in our system ? As remarked in the introductory chapter, a non-linear response could lead to the generation of non-linear fronts, whose speeds depends upon the applied strain. In the main panel of Fig. (6.8), we plot the normalized front speed v_f/c versus the normalized strain rate, γ/γ_c for the random networks at various values of Δz . For $\gamma \gg \gamma_c$, we find $v_f \propto \gamma^{\frac{1}{2}}$. Thus, we find a non-linearity index $n = 2$. This index is consistent with the findings in reference [2], where close to the critical point, the stress response of random spring networks was seen to take the form

$$\sigma = G\gamma + \kappa\gamma|\gamma| \tag{6.15}$$

In the strongly non-linear regime, differentiating once with respect to spatial coordinate x (ignoring the term $G\gamma$), we can write the continuum equation of motion

$$\frac{\partial\sigma}{\partial x} = \rho\frac{\partial^2 y}{\partial t^2}, \tag{6.16}$$

where y is the shear displacement. Using Eq. (6.15), we obtain the non-linear equation

$$\frac{\partial^2 y}{\partial t^2} = \frac{\kappa}{\rho}\frac{\partial\gamma^2}{\partial x}. \tag{6.17}$$

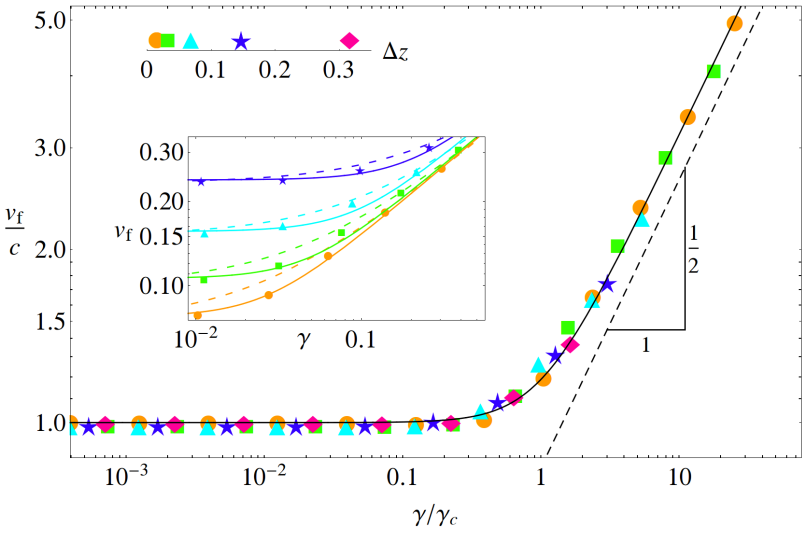

Figure 6.8: In the main panel, the normalized front velocity, v_f/c, is plotted as a function of the normalized strain γ/γ_c for a range of Δz. For $\gamma/\gamma_c \ll 1$, the front speed v_f is independent of the applied strain and corresponds to the linear speed of sound c. In the strongly non-linear regime $\gamma/\gamma_c \gg 1$, the front speed is independent of Δz and scales with the applied strain as $v_f \propto \gamma^{\frac{1}{2}}$ (straight black line). The solid curve is plotted using the relation $v_f = \frac{(G_0^2 + {k_{nl}}^2\gamma^2)^{\frac{1}{4}}}{\sqrt{\rho}}$. The inset compares the solid curves from the main plot to the alternative relation $\tilde{v}_f = \sqrt{c^2 + \frac{k_{nl}\gamma}{\rho}}$ (dashed lines), clearly favouring v_f over $\tilde{v}_f$.

Differentiating once more with respect to x and noting that $\gamma = \frac{\partial y}{\partial x}$, we arrive at the second order non-linear wave equation:

$$\frac{\partial^2 \gamma}{\partial t^2} = \frac{\kappa}{\rho} \frac{\partial^2 \gamma^2}{\partial x^2}. \tag{6.18}$$

Comparing the two terms dimensionally, we can define a characteristic speed

$$v_f \sim \left(\frac{\kappa \gamma}{\rho} \right)^{\frac{1}{2}}. \tag{6.19}$$

In the strongly non-linear regime where the network response persists in the non-quasistatic regime with a front width that spreads super-diffusively, v_f is the only characteristic speed in the system. In essence, this is reminiscent of the effective sound speed we found in Chapter 4, where the effective sound speed depends upon the initial solitary wave energy as $c \sim E^{\frac{1}{10}}$. Since the solitary wave amplitude is related to the energy as $E \sim A^2$, the only characteristic speed in that medium was $c \sim A^{\frac{1}{5}}$. Consequently, one way to understand the response of the random spring network in the strongly non-linear regime is as a simple advection of the super-diffusive fronts with the characteristic speed v_f.

More-over, the critical strain for the transition from linear to non-linear regime can be obtained by comparing the two terms on the right of Eq. (6.15),

$$\gamma_c \sim dz. \tag{6.20}$$

In the main panel of Fig. (6.8), we do find a good collapse of the data, where strains have been normalized by the critical strain Eq. (6.20). Note also, for $\gamma < \gamma_c$ and at later times, the front speed is simply the speed of linear sound $c \sim \sqrt{G}$. Although the dynamics in the intermediate regime $\gamma \sim \gamma_c$ is complex, we do find well defined front propagation and indeed find a good collapse of the data for the front speed by the expression

$$v_f = \frac{\left(G^2 + \kappa^2 \gamma^2 \right)^{\frac{1}{4}}}{\sqrt{\rho}} \tag{6.21}$$

that correctly captures the asymptotic front speeds.